**IOSUD - Universitatea Politehnica Timişoara**
**Şcoala Doctorală de Studii Inginereşti**

# MATERIALS BASED ON $Cd_xZn_{1-x}S$ USED AS VISIBLE LIGHT ACTIVE PHOTOCATALYSTS FOR HYDROGEN PRODUCTION

**PhD Thesis – Summary**

to obtain the scientific title of doctor at the
Polytechnic University of Timisoara
in the field of Materials Engineering
**author Eng. Paula SVERA**
scientific coordinator: Prof.PhD. Eng. Viorel Aurel ŞERBAN
and Prof.PhD.Eng. Nicolae VASZILCSIN
Iulie 2019

## INTRODUCTION

Global population growth along with the development of the technology and energy used has the effect of increasing the environmental pollution and, implicitly, the increasing consumption of fossil fuels. Taking into account the aforementioned, new energy resources are needed, hydrogen having a great potential as energy fuel in the near future. The advantages of hydrogen include the ability to be produced from a variety of raw materials. These include natural gas and coal, as well as renewable resources, such as biomass and water, under the influence of other renewable energies (sunlight, wind energy, or hydro-energy). In this thesis, hydrogen was obtained by photocatalytic decomposition of water, the main advantage of this method being the use of two natural and non-polluting resources, water and sunlight, while the obtained product (hydrogen) has no other co-products.

The main objectives of the thesis involved:

- using a novel Zn source that wasn't utilised in the photocatalytic decomposition process of water with $Cd_xZn_{1-x}S$ type semiconductors;
- synthesis and characterization of $Cd_xZn_{1-x}S$ type materials with the ability to obtain hydrogen;
- designing a installation for hydrogen testing;
- experimental research on the influence of synthesis parameters (the concentration of Zn, the temperature and duration of thermal treatment, the presence of catalyst and organic stabilizer) on the hydrogen production.

## PART I: STUDY OF LITERATURE
## CHAPTER 1 - Characterization of Cd-based photocatalysts

In the photocatalysis process, the photon energy from the higher level of the solar irradiation spectrum, namely the UV and the upper spectrum of the visible spectrum, is converted into chemical energy, more exactly, into hydrogen. Photon energy is proportional to the frequency of solar radiation and is given by $h\nu$, where h is Planck's constant ($6{,}626 \cdot 10^{-34}$ J s) and ν is the frequency [26]. When the photon hits the photocatalytic particle, an electron-hole pair is formed and the generated electrical charge is used to divide the water. In order to reach the water dissociation process, photocatalyst must have appropriate values of the band gap, conduction band

and valence band. In conclusion, generating and separating electron-hole pairs is essential in choosing the photocatalyst. Due to the fact that water does not absorb solar radiation, when splitting the water, it is necessary to include in process a semiconductor with the capacity to efficiently absorb solar energy and separate molecules. The semiconductor, which captures the solar energy, also has the role of generating electrons and holes, which can reduce or oxidize the water molecules adsorbed on the photocatalyst. In this way, during the reaction, photon energy is transformed into chemical energy, a process encountered in photosynthesis, which is why this method is considered artificial [28]. For the direct use of solar radiation in the water splitting process, the photocatalytic material should to be used as a solution, given that water is transparent in the visible field [27].

Generally, photocatalysis involves three essential processes: excitation, material dispersion, and surface transfer of photoinduced carriers [32]. In addition to the above, an efficient catalyst must satisfy several conditions in terms of chemical and semiconductor properties, crystalline structure and morphological texture characteristics. However, there may always be deficient semiconductor characteristics, making it difficult to obtain a photocatalyst whose properties meet all the requirements. One example is the preponderant development of photocatalysts with UV activity and photocatalysts that are active only in the presence of sacrificial agents. Single photocatalysts containing a single component are of no interest due to their low quantum efficiency. However, the hetero-junctions obtained by direct contact between two semiconductors proved to be effective, complex photocatalysts being more investigated than simple photocatalysts [31]. By combining two semiconductors with the corresponding band gap, the lifetime of the fotoinduced carriers can be prolonged, resulting in the amplification of the photocatalytic process [32].

CdS-based photocatalysts are a great potential for photocatalytic hydrogen production due to the narrow band gap and the positioning of the conduction band. More specifically, this compound can absorb visible light and also has the ability to reduce protons to hydrogen. However, this photocatalyst has two major drawbacks: 1) the recombination of photo-excited electrons and holes due to the narrow band gap and 2) the corrosion of the material caused by the photo-excited holes due to the semiconductor instability under the irradiation of light. These disadvantages can be removed by combining CdS with other semiconductors [74-75].

In addition to the high absorption of visible light (2,42 eV), the researchers attempted to improve the photocatalytic efficiency of CdS, one of the methods being the modification of semiconductor nanostructure [77]. The observed increase in yield took place due to the carrier separation efficiency, carrier velocity of electrons, and response velocity of electrons at the interface of CdS nanostructures [78]. Metallic oxides, which are specific for having broad band gaps and the inability to absorb visible light from the light spectrum, are also very stable in photocatalytic processes. By combining a metal oxide with CdS, a better-performing photocatalyst can be obtained, one example being the ZnO and CdS nanostructures [79-81].

Another method of improving CdS involves changing material morphology in various forms [85-86], such as nanocrystals [87], nanowires [88] and nanostructures [89] or by combining with metallic sulphides. From the metal sulfides, ZnS attracted the most attention due to the ability to form solid CdS solutions with better quantum efficiency [90]. An example of this is the solid solution $(Zn_{0.95}Cu_{0.05})_{1-x}Cd_xS$. For the same compound, Cd concentrations have been modified in order to obtain better efficiency in the presence of $SO_3^{2-}$ and $S_2^{2-}$ ions and under the irradiance of visible light. This solid solution contains nanocrystals of 2-5 nm and has a band gap of 2 eV [90]. There are semiconductors that have the ability to sustain only one of the water decomposition reactions (water reduction or oxidation reaction) in the presence of suitable sacrificing agents (electron donors or acceptors). Usually, sacrificial agents react with one of the photo-induced carriers, while others react with water, producing hydrogen or oxygen. Electrons resulting from the formation of holes on the surface of the semiconductors during the excitation are used for the water reduction reaction, and the captured electrons are the ones resulting in the water oxidation reaction. Generally, electron donors are much more easily oxidized by the excited holes than by water, and electron acceptors are much easier to reduce by water than by excited electrons. The most common

electron donors are methanol, ethanol, triethanolamine (TEA) and $Na_2S$ / $Na_2SO_3$ solutions, while the metal cations $Ag^+$ and $Fe^{3+}$ are electron acceptors [39].

In the water splitting process, addition of catalyst has the intent to intensify the oxidation of water or reducing the reactions that take place. The most commonly used catalysts in water decomposition are metallic nanoparticles that form semiconductor junctions and implicitly enhance the separation of carrier charges within the photocatalyst or photoelectrochemical cell. In principle, the contact between the metal and the semiconductor creates an electric field that separates the excited electrons and holes much easier. If the metal is compatible with the conductor band of the semiconductor, the electrons excited pass from the semiconductor to the metal and from there can react with water [49]. Due to the small overcapacity, the metal has the ability to provide active centers for generating hydrogen in the water reduction reaction.

The physical and chemical properties of the catalyst, such as particle size or valence state, are dependent on the deposition method which implicitly affects the performance of hydrogen production [31]. Even if the deposition of several catalysts would generate more active areas, their presence would reduce the absorption capacity of the photocatalyst. Concentration of the catalyst must therefore be optimized to achieve the maximum possible decomposition of water under the influence of light. Another important element that influences the water decomposition process is the photocatalytic system. When water is decomposed, semiconductor photocatalysts are used in the form of particles or powders suspended in aqueous solutions [34], the operation of these systems is based on the fact that each photocatalyst particle acts as a microelectrod, which performs both oxidation and water reduction, precisely photo-oxidation takes place at the n-type semiconductor and photo-reduction at the semiconductor *p* (Figure 1). Systems of this type are cheaper and easier to achieve than photoelectrochemical cells. Also, another advantage is that it does not require high electrical conductivity, as is the case with the photoelectrochemical cell. In addition, the efficiency of light absorption in powder suspensions can reach a very high level due to the exposure to light of a large surface of the semiconductor. The disadvantage of these systems is the lower efficiency of load carriers compared to electrochemical systems.

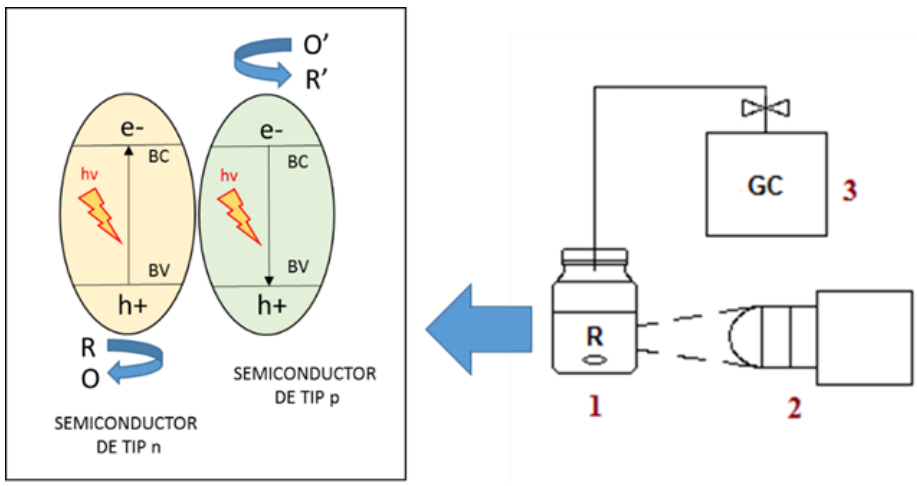


Figure 1 - Representation of the general water decomposition mechanism in the photocatalysis process together with the basic components of the installation: 1-reactor; 2- light source; 3-gas chromatograph

## PART II - Original contributions
## CHAPTER 2 - Experimental Materials and Methods

This chapter describes the materials and methods used for the synthesis of CdS precursors and $Cd_xZn_{1-x}S$ photocatalysts. All the materials obtained were hydrothermaly treated, the used autoclave being represented in Figure 2.

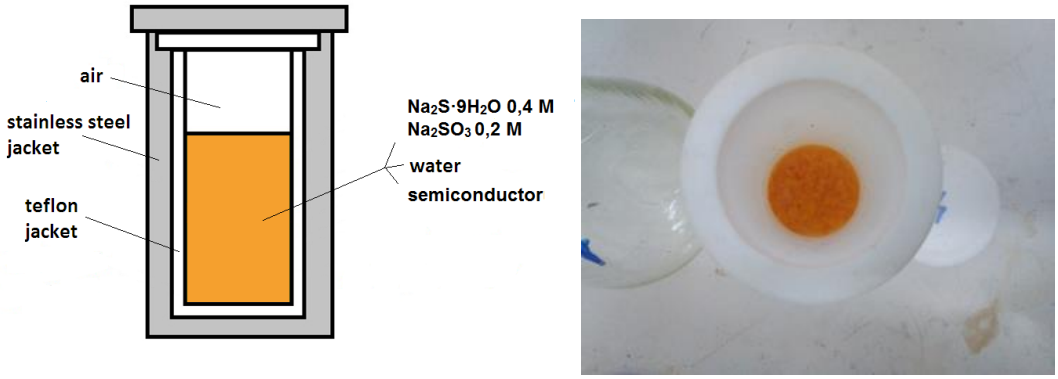


Figure 2 - Schematic representation (left) and image (right) of the autoclave used for material synthesis

Synthesis of precursors started from the production of cubic, hexagonal and cubic-hexagonal crystalline phase materials in order to determine the best hydrogen yields obtained by gas chromatographic testing and, implicitly, to continue the research from the best performing precursor. Photocatalysts were obtained at different Zn concentrations, temperature and duration of thermal treatment, as well as in the presence of the catalyst and the organic stabilizer.

In the study was designed a real-time hydrogen testing system, which was connected to the gas chromatograph, and also in the first part of the study, the installation was connected to a burette for preliminary material testing, a much faster method to demonstrate the photo activity of the materials.

The test procedure for both the burette-connected plant and the gas chromatograph-connected installation consisted of a reactor filled with 100 mL of 0.4 M $Na_2S \cdot 9H_2O$ and 0.2 M $Na_2SO_3$ solution and 0.05 g photocatalyst, which was then sealed, exposed to agitation and placed in the air recirculation box (equipped with a cooling fan) in order to maintain constant temperature. A xenon bulb (300 W) with focused light on the reactor was used as a light source. The reactor was connected via a vacuum pump loop, gas cylinder (nitrogen or argon) and burette or gas chromatograph. The following step was to ultrasonicate the reactor and system vacuuming, and then the introduction of the gas into the system to create the inert atmosphere. In the case of preliminary burette test hydrogen, the downward movement of the burette indicates the presence of the formed gas, and by comparing several samples it was possible to check the higher or lower activity of the photocatalyst tested before testing on the gas chromatograph.

The materials were analyzed using nine methods of characterization:

-X-ray diffraction, XRD
-UV-VIS spectroscopy, UV-VIS
-Raman spectroscopy
-Scanning Electron Microscopy, SEM
-Electronic Transmission Microscopy, TEM
-X-ray dispersion spectroscopy, EDAX
-Fluorescence spectrometry
-Brunauer-Emmet-Teller Method, BET
-Gas-chromatography, GC

## CHAPTER 3 - Characterization and examination of precursors and photocatalytic materials obtained using Zn $(NO_3)_2 \cdot 6H_2O$ as Zn source

The three CdS precursors with preponderent cubic (CdS42), hexagonal (CdS15) and cubic-hexagonal phase (CdS7) were analyzed, with the best precursor being used further in the photocatalysis study.

Specific patterns observed in the XRD spectrum confirmed the presence of the target crystalline phases (Figure 3 left):

- (1 0 0) (0 0 2) (1 0 1) (1 0 2) specific for hexahedral phase were obtained for CdS 15 sample according to JCPDS Nr. 00-001-0780;
- (1 1 1) (2 0 0) (2 2 0) (3 3 1) specific for cubic phase were obtained for CdS 42 sample according to JCPDS No. 00-002-0454.

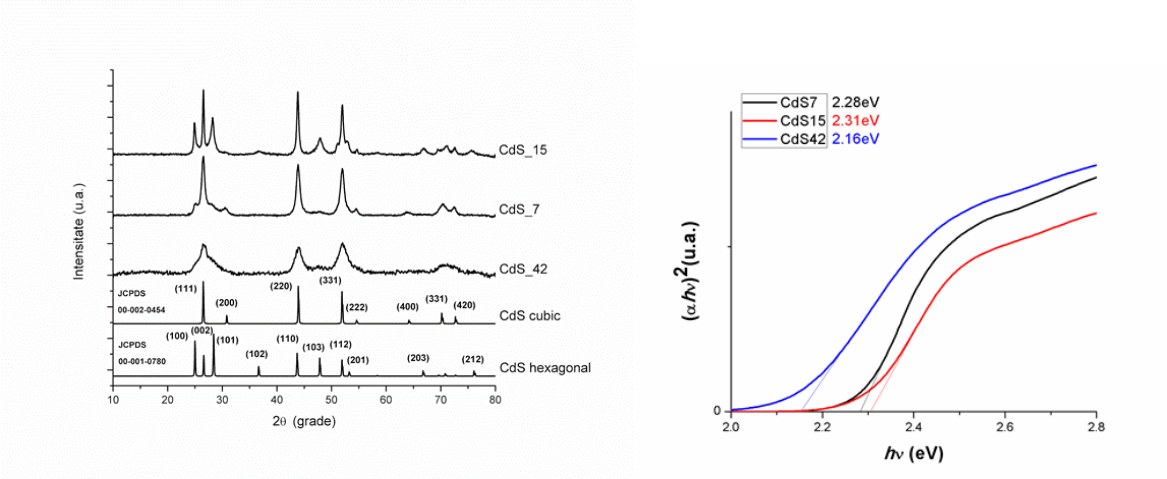


Figure 3 - XRD Spectra (Left) and band gaps (Right) of CdS Precursors

The calculated band gaps (Figure 3 right) for the CdS7, CdS15 and CdS42 samples have values of 2.28 eV, 2.31 eV and 2.16 eV respectively, similar to those obtained in literature. The band gap value of 2 eV, which corresponds to the infrared range in the spectrum, is very unstable, the photocorrosion process taking place during the photocatalysis, so that from the photocatalytic point of view, the band gap can anticipate the compound with better hydrogen production. It is also observed the displacements to higher values of the band gaps of materials due to the increase in volume and due to the electronegativity of the constituent elements.

Table 1 - Volumetric (Left) and Gas Chromatographic (Right) Test Results for CdS7, CdS15 and CdS42

| Sample | Volume of water from the burette [mL] |
|---|---|
| CdS7 | 5,8 |
| CdS15 | 6,2 |
| CdS42 | 3,5 |

| Sample | $H_2$ [mmol $g^{-1}$ $h^{-1}$] |
|---|---|
| CdS7 | 0,00060 |
| CdS15 | 0,00063 |
| CdS42 | 0,00032 |

Volumetric and low gas chromatographic results of CdS42 were previously confirmed by band gap values obtained from UV absorption spectra, from which the importance of band gaps in the study of photo-catalytic materials can be concluded. Also, the importance of the crystalline structures present in the materials have been demonstrated, in this case the crystalline hexagonal and hexagonal-cubic structure showed the best results both in the volumetric test and in the gas chromatographic analysis (Table 1).

## CHAPTER 4 - Characterization and examination of photocatalytic materials obtained using $ZnSO_4 \cdot 7H_2O$ as Zn source

The phase difference of the semiconductor materials causes changes at the level of electrical bands, influencing the photochemical, photocatalytic and photophysical properties. It should be noted, however, that the crystalline structure is strongly influenced by the preparation conditions (Figure 4). It can be observed that the $Cd_xZn_{1-x}S$ nanoparticles exhibit shifts of the diffraction lines

to higher values of the angle 2θ with increasing zinc content. This phenomenon can be explained by the fact that the $Zn^{2+}$ ionic radius (0.74 Å) is much smaller than that of $Cd^{2+}$ (0.97 Å), the substitution of $Zn^{2+}$ ions in CdS causing the d-spacing to decrease, and thus the displacement of the diffraction lines. Also, the successive displacement of the diffraction lines demonstrates the formation of the solid solution of $Cd_xZn_{1-x}S$ and not just a mixture of ZnS and CdS. Regarding the thermal treatment of photocatalytic materials, it was observed that the characteristic line diffraction pattern (2 0 0) specific for the CdS cubic phase as well as the (100) and (102) diffraction lines specific to the hexagonal CdS phase increase in intensity with increasing temperature. From the cubic ZnS specific crystalline phase, an increase in the intensity of the temperature for the specific diffraction line (3 1 1) is also observed.

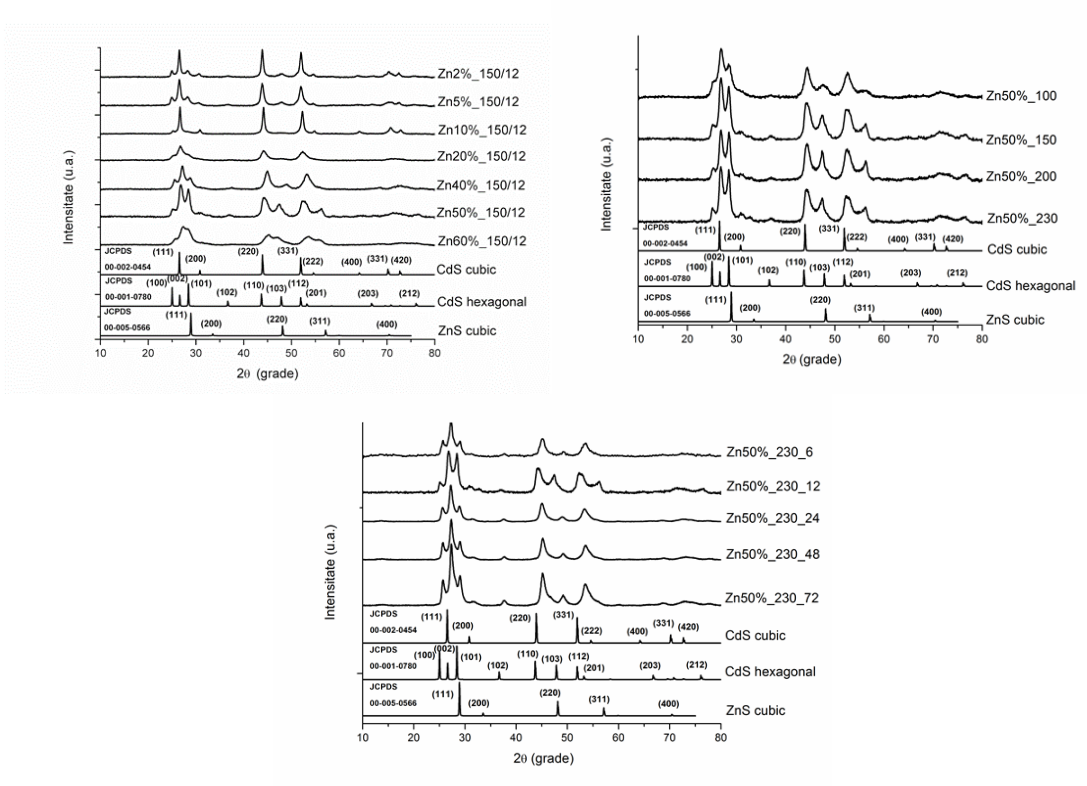


Figure 4 - XRD spectra of photocatalysts at different Zn concentrations (left), different temperatures (right) and different heat treatment periods (down)

Band gap values for compounds with different Zn concentrations are in the range of 2.20 to 2.56 eV (Figure 5). However, the movement of the band gap to blue is not symmetrical with the Zn content increase, involving very small differences. With temperature changes, the values of the band gaps are between 2.36 eV - 2.38 eV (Figure 6). It has been observed that the values of the band gaps tend to increase with the increase in the duration of the hydrothermal treatment, an effect due to defects in the photocatalytic particles which implicitly influence the scattering of the light.

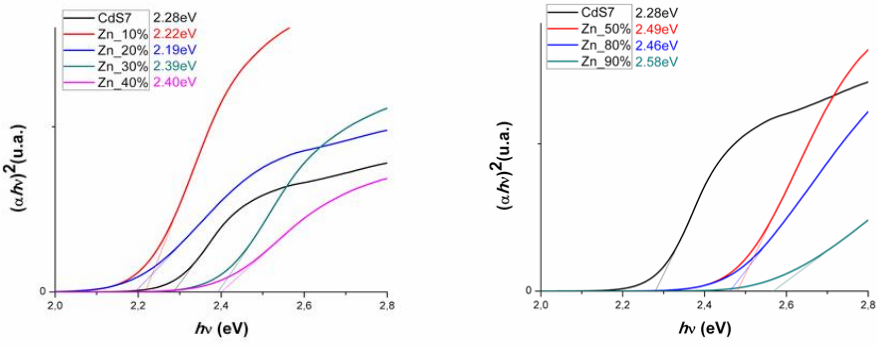


Figure 5 – Band gaps of photocatalysts with different Zn concentrations

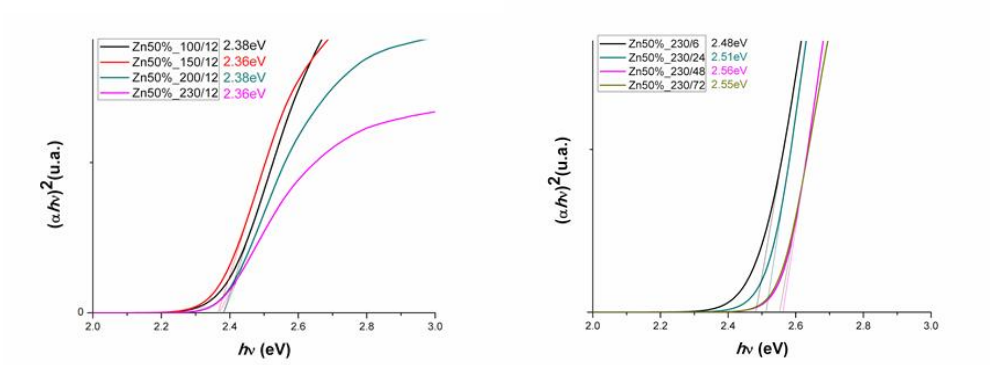


Figure 6 - Forbidden bands of calculated photocatalysts at temperatures (left) and different heat treatment periods (right)

Adsorption-desorption isotherms were disclosed in order to assess the morphological properties of materials by varying the Zn concentration, temperature, and exposure to heat treatment. From the isotherms were extracted the morphological parameters, noticing that the largest specific area between compounds with a different concentration of Zn was recorded for the Zn50% _150 / 12 sample having a specific surface area of 76.0 $m^2g^{-1}$ and the smallest specific area with a value of 27.5 $m^2g^{-1}$ was obtained for the Zn20% _150 / 12 sample; Zn20% _150 / 12 also indicates the smallest total pore volume (VTP). Comparing the hydrothermal treated materials at different temperatures, Zn50% _230 / 12 shows the highest specific area of 74.7 $m^2g^{-1}$ and Zn50% _100 / 12 the lowest specific surface area of 23.6 $m^2g^{-1}$. It should be noted, however, that the temperature influences the total pore volume and the specific surface. Zn50% _230 / 12 is also evidenced by orderly porosity, which is not the case with other samples. By comparing materials exposed to thermal treatment with different time duration, it was concluded that the specific surface area and total pore volume decreased with increasing time, and the pore size calculated by the DFT method also decreased. It can be noticed that the roughness of the materials increases with the increase in the duration of the heat treatment. By comparing the sample Zn50% _230 / 48 with the sample Zn50% _230 / 72, it is noted that both materials exhibit orderly porosity, the sample Zn50% _230 / 72 having pores much more ordered.

Table 2 – Gas-chromatographic values of photocatalysts with different Zn concentration (left), temperature (top right) and different thermal treatment periods (bottom right)

| Sample | $H_2$ [mmol $g^{-1}$ $h^{-1}$] |
|---|---|
| Zn2%_150/12 | 0,028 |
| Zn5%_150/12 | 0,018 |
| Zn10%_150/12 | 0,014 |
| Zn20%_150/12 | 0,024 |
| Zn40%_150/12 | 0,039 |
| Zn50%_150/12 | 0,128 |
| Zn60%_150/12 | 0,125 |

| Sample | $H_2$ [mmol $g^{-1}$ $h^{-1}$] |
|---|---|
| Zn50%_100/12 | 0,032 |
| Zn50%_150/12 | 0,128 |
| Zn50%_200/12 | 0,112 |
| Zn50%_230/12 | 0,543 |

| Sample | $H_2$ [mmol $g^{-1}$ $h^{-1}$] |
|---|---|
| Zn50%_230/6 | 0,275 |
| Zn50%_230/24 | 0,320 |
| Zn50%_230/48 | 0,634 |
| Zn50%_230/72 | 0,702 |

By comparing the obtained gas-chromatographic results (Table 2), the Zn50% _150 / 12 compound exhibits the highest specific surface area from the category of materials obtained at different Zn concentrations, having also the best photocatalytic yield.

The increasing thermal treatment period positively influences the increase in hydrogen production efficiency. Looking at the nitrogen adsorption / desorption isotherms using the DFT method, we can see that the decrease in particle size-similar samples with zinc concentration variations and thermally treated samples at different temperatures can significantly improve hydrogen production.

## CHAPTER 5 - Conclusions

The reported doctoral study had the main purpose to obtain materials with photocatalytic activity for water splitting. The first step of the experimental part consisted in the synthesis of CdS with different crystalline phases and the identification of the most prestigious material in the photocatalytic process by testing. All photocatalysts obtained in this study are based on CdS to which was added the second Zn-based semiconductor. The source of Zn was also investigated, confirming that $ZnSO_4 \cdot 7H_2O$ is more suitable for obtaining hydrogen. The next step was to change the synthesis temperature and the heat treatment time. In the last stage of the experimental part, the catalyst and the stabilizer were added in order to determine their influence on the hydrogen production. The final results demonstrate the importance of the catalyst, by increasing the hydrogen production from 0.70 mmol $g^{-1}$ $h^{-1}$ to 1.99 mmol $g^{-1}$ $h^{-1}$. By adding the catalyst, another phenomenon was observed, namely the decrease of the specific surface.

The final results of the PhD study compared to other researches in the field bring to the knowledge the following accounts:

-The XRD spectra of the studied materials confirm the crystallinity of the compounds;

-GC analysis has demonstrated hydrogen production under irradiation of light in the visible spectra;

-BET analyzes have shown the importance of pore distribution and pore size, especially for photocatalysts with different heat treatment;

-Best photocatalysts were tested in the presence of a Pd catalyst resulting in the best photocatalytic performance obtained from Zn50% _230 / 72P prepared at 230 ° C for 72 hours with 50% Zn and in the presence of the Pd catalyst.

## REFERENCES:


[26] C. Acar, I. Dincer, G.F. Naterer, Review of photocatalytic water-splitting methods for sustainable hydrogen production, Int. J. Energy Res. 40 (2016) 1449-1473.

[28] K.S. Kang, C.H. Kim, W.C. Cho, K.K. Bae, S.H. Kim, C.S. Park, Novel two-step thermochemical cycle for hydrogen production from water using germanium oxide: KIER 4 thermochemical cycle, Int. J. Hydrogen Energy 34 (2009) 4283–4290.

[27] I. Marin, Akademos Revistă de ştiinţă, inovare, cultură şi artă, 3 (46) (2017) 56-59 ISSN 1857-0461.

[32] F. Gaspari, Comprehensive Energy Systems, 2.10 Semiconductors, Volume 2, Elsevier (2018) 266-302.

[31] M.R. Gholipour, C.T. Dinh, F. Beland, T.O. Do, Nanocomposite heterojunctions as sunlight-driven photocatalysts for hydrogen production from water splitting, Nanoscale 7 (2015) 8187–8208.

[34] A.J. Bard, Photoelectrochemistry and heterogeneous photo-catalysis at semiconductors, J. Photochem. 10 (1979) 59–75.

[39] J. Schneider, D.W. Bahnemann, Undesired Role of Sacrificial Reagents in Photocatalysis, J. Phys. Chem. Lett., 4 (20) (2013) 3479–3483.

[49] J.S. Jang, S.H. Choi, H. G. Kim, J.S. Lee, Location and State of Pt in Platinized CdS/TiO2 Photocatalysts for Hydrogen Production from Water under Visible Light, J. Phys. Chem. C 112 (2008) 17200–17205.

[74] P. Svera, A.V. Racu, C. Mosoarca, D. Ursu, P.A. Linul, R. Baies, R. Banica, Influence of precursor crystallinity on photocatalytic activity of PdS/CdS-ZnS, J. Optoelectron. Adv. M. 18

(2016) 1027 – 1032.
[75] P. Svera, D. Niznansky, M.N. Stefanut, D.Ursu, P. Sfirloaga, A. Dabici, B.O. Taranu, A.M. Putz, V.A. Serban, Studies on the hydrothermal synthesis of CdxZn1-xS compounds, Processing and Application of Ceramics 12 (2018) 287–294.
[77] D. Jing, L. Guo, A Novel Method for the Preparation of a Highly Stable and Active CdS Photocatalyst with a Special Surface Nanostructure, J. Phys. Chem. B 110 (2006) 11139–11145.
[78] J. Cao, J.Z. Sun, J. Hong, H.Y. Li, H.Z. Chen, M. Wang, Carbon Nanotube/CdS Core-Shell nanowires Prepared by a simple room-temperature chemical reduction method, Adv. Mater. 16 (2004) 84–87.
[79] S. Huang, Y. Lin, J.H. Yang, Y. Yu, CdS-Based Semiconductor Photocatalysts for Hydrogen Production from Water Splitting under Solar Light, in Nanotechnology for Sustainable Energy, ACS Symposium Series (2013) 219-241.
[80] X. Wang, G. Liu, G.Q. Lu, H. M. Cheng, Stable photocatalytic hydrogen evolution from water over ZnO-CdS core–shell nanorodsInt, J. Hydrogen Energy 35 (2010) 8199–8205.
[81] Y. Chen, L. Guo, Highly efficient visible-light-driven photocatalytic hydrogen production from water using Cd0.5Zn0.5S/TNTs (titanate nanotubes) nanocomposites without noble metals, J.Mater.Chem. 22 (2012) 7507–7514.
[85] S. Rengaraj, S. Venkataraj, S.H. Jee, Y. Kim, C.Tai, E. Repo, A. Koistinen, A. Ferancova, M. Sillanp, Cauliflower-like CdS Microspheres Composed of Nanocrystals and Their Physicochemical Properties, Langmuir 27 (2011) 352–358.
[86] S. Kudera, L. Carbone, L. Manna, W.J. Parak, Growth mechanism, shape and composition control of semiconductor nanocrystals, in Semiconductor Nanocrystal Quantum Dots, Springer (2008) 1-34.
[87] ] Z. Shen, G. Chen, Q. Wang, Y. Yu, C. Zhou, Y. Wang, Sonochemistry synthesis and enhanced photocatalytic H2-production activity of nanocrystals embedded in CdS/ZnS/In2S3 microspheres, Nanoscale 4 (2012) 2010–2017.
[88] Z. Khan, T. R. Chetia, M. Qureshi, Rational design of hyperbranched 3D heteroarrays of SrS/CdS: synthesis, characterization and evaluation of photocatalytic properties for efficient hydrogen generation and organic dye degradation, Nanoscale 4 (2012) 3543–3550.
[89] U. Gupta, B.G. Rao, U. Maitra, B.E. Prasad, C.N.R. Rao, Visible-Light-Induced Generation of H2 by Nanocomposites of Few-Layer TiS2 and TaS2 with CdS Nanoparticles, Chem. – Asian J. 9 (2014) 1311–1315.
[90] W. Zhang, Z. Zhong, Y. Wang and R. Xu, Doped Solid Solution: (Zn0.95Cu0.05)1−xCdxS Nanocrystals with High Activity for H2 Evolution from Aqueous Solutions under Visible Light, J. Phys. Chem. C 112 (2008) 17635–17642.